

Dynamic Response Bound Estimation of Structures with Interval Parameters

Janaína CV Albuquerque* and José Juliano De L Junior

Institute of Mechanical Engineering, Federal University of Itajubá, Brazil

Abstract

This study aims to evaluate the result of mechanical vibration problems in presence of an interval of values for parameters such as mass, length, modulus of elasticity, moment of inertia. A possibility and computationally efficient method is proposed to obtain the limits of natural frequency of systems with interval parameters. The interval eigenvalue problem is formulated by the Finite Element Method (FEM) which stiffness and mass matrices are submitted to disturbance by Perturbation Theory of Matrices (PTM). At each stage of the analysis, the existence of uncertainty in matrix formulation is considered as the presence of disorder in a pseudo-deterministic system capable of providing technically reliable and efficient results. Numerical results are presented using a tool developed by the author in MATLAB®. This program works with dynamic structures with interval uncertainty. The numerical results are compared with the literature and with a Monte Carlo simulation. Experimental tests were conducted to validate the results of the proposed method.

Keywords: Interval parameters; Eigenvalue; Perturbation theory of matrices; Monte Carlo method

Introduction

The behavior of structures with interval (or uncertain) parameters has been investigated by several authors due to their importance in the fields of structural mechanical engineering. The presence of interval parameters in mechanical designs can be attributed to physical imperfections, inaccuracies of the mathematical model and the complexity of the system. The evaluation of project uncertainties has become a stage that requires increasingly attention and special care during its elaboration to guarantee technically reliable projects with a high degree of safety and low financial costs. Uncertainty is defined as a deficiency that may or may not occur during the structural modeling process due to the engineer's lack of knowledge about the design, according to Oberkampf [1]. They arise due to incompatibilities and inaccuracies in physical and geometric parameters, such as load, modulus of elasticity, Poisson's coefficient, length and others.

One way to represent and perform operations with inaccurate data is to use interval arithmetic. In this context, an uncertainty can be represented by a range of real numbers, which contains the exact unknown value. In this way, uncertainty is involved by the limits of the interval and there is no need to know the probability distribution to represent it. Burkill [2] introduced the first approach to interval arithmetic. Sunaga [3,4] concretized the use of arithmetic interval years later. But it was with Moore [5] doctoral thesis that interval arithmetic gained special attention, in which the author presents a modern development of the technique with a range of practical use options.

Landowski [4] presented a comparison of Moore interval arithmetic and Relative Distance Measure (RDM) interval arithmetic. Also, in both Moore and RDM arithmetic the basic operations and their properties are described. Solved examples show that the results obtained using the RDM arithmetic are multidimensional while Moore arithmetic gives one dimensional solution. The Monte Carlo method is a well-known methodology and widely used to validate new uncertainty treatment techniques in mechanical systems, but its high computational cost makes it unfeasible to solve some problems. Several authors have used the Perturbation Technique to evaluate uncertainties in the structural response to avoid problems caused by improper use of the Monte Carlo method. Matos [6] uses the technique in civil engineering to evaluate

the response of structural systems with interval parameters, through the mean values and their standard deviations.

Matsumoto e Iwaya [7] presented two methodologies to solve truss problem with uncertainties in structure geometry. In the first methodology, the problem is formulated by FEM adapted to interval arithmetic. In the second methodology, the FEM is formulated as an optimization problem, which proved to be more efficient, since the answers that came closer to the true solution obtained by Monte Carlo simulation. The analysis of uncertainties in oil exploration is an area of interest to companies to reduce the exploratory risk with the consequent optimization of financial resources. Considering this scenario, Pereira [8] presented a study with the use of interval arithmetic and fuzzy arithmetic as an alternative to evaluate the uncertainty in numerical methods for basin modeling. The rigid-flexible multibody system is meshed by using a unified mesh of the absolute nodal coordinate formulation (ANCF). Interval eigenvalue problems were studied by Qiu [9]. The authors interested in structural vibration problems with interval variables applied the Parameter Solution Vertex Theorem in the interval eigenproblems solution. Qiu [9] worked with positive decomposition of stiffness and mass matrices. Wang [10] proposed a non-intrusive computation methodology to study the dynamics of rigid-flexible multibody systems with a large number of uncertain interval parameters.

Methods

Interval arithmetics

In general, the uncertainties can be divided into three types: stochastic analysis, fuzzy analysis and interval analysis.

*Corresponding author: Albuquerque JCV, Institute of Mechanical Engineering, Federal University of Itajubá, Brazil, Tel: (31) 3839-0800; E-mail: jana_cvaz@yahoo.com.br

Received May 10, 2018; Accepted March 16, 2018; Published March 21, 2018

Citation: Albuquerque JCV, De L Junior JJ (2018) Dynamic Response Bound Estimation of Structures with Interval Parameters. J Appl Mech Eng 7: 306. doi:10.4172/2168-9873.1000306

Copyright: © 2018 Albuquerque JCV, et al. This is an open-access article distributed under the terms of the Creative Commons Attribution License, which permits unrestricted use, distribution, and reproduction in any medium, provided the original author and source are credited.

- **Stochastic analysis:** the stochastic approach to uncertain problems is to model the structural parameters as random quantities. Therefore, all information about the structural parameters is provided by the probability density functions. This probability density function is then used to determine an estimate of the system's behavior.
- **Fuzzy analyses:** The fuzzy approach to the uncertain problems is to model the structural parameters as fuzzy quantities. In conventional set theories, either an element belongs or does not belong to set. However, fuzzy sets have a membership function that allows for "partial membership" in the set. Using this method, structural parameters are quantified by fuzzy sets.
- **Interval analysis:** The interval approach to the uncertain problems is to model the structural parameters as interval quantities. In this method, the uncertainty in the elements is viewed by a closed set-representation of element parameter that can vary within intervals between extreme values. Then, structural analysis is performed using interval operations.

In the interval analysis, a subset of real numbers \mathfrak{R} represented by \tilde{X} (see Equation (1)) is called a closed real interval or simply an interval. The symbol (\sim) represents interval parameters. The boundaries of the interval are represented by: l , lower bound, and u , upper bound.

$$\tilde{X} = [x^l; x^u] = \{x : x^l \leq x \leq x^u, x^l, x^u \in \mathfrak{R}\} \quad (1)$$

The median value of interval number \tilde{X} can be defined as:

$$X^c = \frac{x^l + x^u}{2} \quad (2)$$

The radius value of interval number \tilde{X} can be defined as:

$$\tilde{X}^R = \varepsilon \left(\frac{x^u - x^l}{2} \right), \quad \varepsilon = [-1; 1] \quad (3)$$

An interval number can also be written as summation of center and radial values. This representation is called centered formulation and can be redefined as:

$$\tilde{X} = X^c + \tilde{X}^R \quad (4)$$

Some valid algebraic rules for real numbers remain valid for interval numbers. The rules of equality for real numbers are not valid for interval numbers, only the inclusions rules are valid. There are two basic rules in interval arithmetic:

- Two equivalent arithmetic expressions in real arithmetic are equivalent in interval arithmetic, if and only if the expression variables appear only once on each side of the equality.
- If $f(x)$ and $g(x)$ are two equivalent arithmetic expressions in real arithmetic, so the inclusion $f(x) \subseteq g(x)$ is true, if and only if all the variables of the expression appear only once in $f(x)$.

For example, these two basic rules are showed as follows.

$$f(x) = \frac{1}{1 + \frac{1}{x}} \quad \text{with } x \neq 0 \quad (5)$$

In conventional arithmetic, equation (5) is equivalent to the simplified formula given in equation (6).

$$g(x) = \frac{x}{x+1} \quad (6)$$

Substituting interval variable $x = [2; 3]$ into equations (5) and (6), the functions can be given as follows.

$$f([2; 3]) = \frac{1}{1 + \frac{1}{[2; 3]}} = \frac{1}{1 + \left[\frac{1}{3}; \frac{1}{2} \right]} = \frac{1}{\left[\frac{4}{3}; \frac{3}{2} \right]} = \left[\frac{2}{3}; \frac{3}{4} \right] \quad (7)$$

$$g([2; 3]) = \frac{[2; 3]}{([2; 3] + 1)} = \frac{[2; 3]}{[3; 4]} = [2; 3] \times \left[\frac{1}{4}; \frac{1}{3} \right] = \left[\frac{1}{2}; 1 \right] \quad (8)$$

The inclusion property is valid in equations (7) and (8), if $f(x) \subseteq g(x)$. The variable x from function $g(x)$ appears twice and, in this case, $g(x)$ generates as a result an interval greater than $f(x)$, confirming an inadequate overestimation in equation (8) where variable repetition occurs.

Perturbation theory of matrix applied to problems of eigenvalues with interval parameters classic eigenvalue problem

$$[A]\{x\} = \lambda\{x\} \quad (9)$$

where $[A]$ is a symmetric matrix of order p , λ is eigenvalue and $\{x\}$ is associated eigen-vector

Pre-multiplying equation (9) by $\{x\}^T$, the eigenvalue problem turns:

$$\{x\}^T [A]\{x\} = \lambda \{x\}^T \{x\} \quad (10)$$

Equation (10) can be rearranged in the ratio known as Rayleigh quotient, according to Equation (11). The Rayleigh quotient defines the largest and the smallest eigenvalue of a symmetric matrix.

$$R(x) = \frac{\{x\}^T [A]\{x\}}{\{x\}^T \{x\}} \quad (11)$$

It can be shown that, for a symmetric matrix, the Rayleigh quotient is limited between the smallest, and the largest, eigen-value.

$$\lambda_1 \leq R(x) \leq \lambda_p \quad (12)$$

The first eigenvalue λ_1 can be obtained by unrestricted minimization of equation (11) as follows.

$$\min_{\substack{\{x\} \in R^p \\ \{x\} \neq \{0\}}} R(x) = \min_{\substack{\{x\} \in R^p \\ \{x\} \neq \{0\}}} \left(\frac{\{x\}^T [A]\{x\}}{\{x\}^T \{x\}} \right) = \lambda_1 \quad (13)$$

The other eigenvalues are obtained by applying the additional constraints, $\{x\}^T \{s_i\} = 0$, $\{x\} \neq \{0\}$ e $i = 1, \dots, p$, as can be

shown in equation (14). The eigenvector, $\{x\}$, must be perpendicular to an arbitrary vector, $\{s\}$. The imposition of perpendicularity ensures

$$\text{that the internal product of the vectors is null } \left(\{x\}^T \{s\} = 0 \right). \quad (14)$$

Symmetric positive semidefinite matrix

The symmetric matrix $[A]$ can be disturbed by a symmetric, positive semidefinite matrix $[E]$ which has the following property.

$$\{x\}^T [E]\{x\} \geq 0 \quad \text{for } \{x\} \neq \{0\} \in \mathfrak{R} \quad (15)$$

Comparing the Rayleigh quotient of the symmetric matrix $[A]$ with the quotient of the disturbed symmetric matrix $[[A]+[E]]$ one obtains the following inequality:

$$\frac{\{x\}^T [[A]+[E]]\{x\}}{\{x\}^T \{x\}} \geq \frac{\{x\}^T [A]\{x\}}{\{x\}^T \{x\}} \quad (16)$$

The first eigenvalue of a disturbed matrix is the solution of equation (17):

$$\min_{\substack{\{x\} \in \mathbb{R}^p \\ \{x\} \neq \{0\}}} \left(\frac{\{x\}^T [[A]+[E]]\{x\}}{\{x\}^T \{x\}} \right) \geq \min_{\substack{\{x\} \in \mathbb{R}^p \\ \{x\} \neq \{0\}}} \left(\frac{\{x\}^T [A]\{x\}}{\{x\}^T \{x\}} \right) \quad (17)$$

The other eigenvalues are obtained by solving the equation (18):

$$\max_{\substack{\{x\}^T \{s_i\} = \{0\} \\ i=1, \dots, p \\ \{x\} \neq \{0\}}} \left(\frac{\{x\}^T [[A]+[E]]\{x\}}{\{x\}^T \{x\}} \right) \geq \max_{\substack{\{x\}^T \{s_i\} = \{0\} \\ i=1, \dots, p \\ \{x\} \neq \{0\}}} \left(\frac{\{x\}^T [A]\{x\}}{\{x\}^T \{x\}} \right) \quad (18)$$

The eigenvalues of a symmetric matrix subject to a positive semidefinite perturbation monotonically increase from the eigenvalues of the exact matrix.

$$\hat{\lambda}_i([A]+[E]) \geq \lambda_i([A]) \quad (19)$$

Similarly, all eigenvalues of a symmetric matrix subject to a negative semidefinite perturbation monotonically decrease from the eigenvalues of the exact matrix.

$$\hat{\lambda}_i([A]-[E]) \leq \lambda_i([A]) \quad (20)$$

Eigenvalue problem in dynamic structures

The classic problem of generalized eigenvalue for dynamic structures is shown in equation (21). The assembly of stiffness matrix $[K]$ and mass matrix $[M]$ can be obtained by finite element method.

$$[K]\{x\} = \lambda[M]\{x\} \quad (21)$$

where $[K]$ is the global stiffness matrix and $[M]$ is the global mass matrix.

Similarly, to equation (21), the problem of generalized interval eigenvalue for dynamic structures can be obtained by replacing the stiffness matrix and mass matrix by interval matrices $[\tilde{K}]$ and $[\tilde{M}]$, according to equation (22).

$$[\tilde{K}]\{\tilde{x}\} = \tilde{\lambda}[\tilde{M}]\{\tilde{x}\} \quad (22)$$

where $\tilde{\lambda}$ is the interval eigenvalue defined by $\tilde{\lambda} = [\lambda^l, \lambda^u]$.

$$[\tilde{K}]\{\tilde{x}\} = (\tilde{\omega}_p^2)[\tilde{M}]\{\tilde{x}\} \quad (23)$$

$$\left(\sum_{i=1}^p ([l_i, u_i]) [\bar{K}_i]^e \right) \{\tilde{x}\} = (\tilde{\omega}_i^2) \left(\sum_{i=1}^p ([l_i, u_i]) [\bar{M}_i]^e \right) \{\tilde{x}\} \quad (24)$$

where $\{\tilde{x}\}$ is the interval mode shape and $\tilde{\omega}_p$ is the interval natural frequency that is obtained by $\tilde{\omega}_i = \sqrt{\tilde{\lambda}_i}$, l_i is the lower bound of matrix elements and u_i is the upper bound, $[\bar{K}_i]^e$ e $[\bar{M}_i]^e$ are deterministic matrix for each element of the discretized structure.

The interval-eigenvalue problem, as shown in equation (23), can be transformed into a pseudo-deterministic eigenvalue problem as equation (25) subject to a perturbation matrix by introducing the central perturbation matrix and the radial perturbation matrix.

$$([K^C] + [\tilde{K}^R])\{\tilde{x}\} = \tilde{\omega}_i^2 ([M^C] + [\tilde{M}^R])\{\tilde{x}\} \quad (25)$$

$$[\tilde{M}] = [M^C] + [\tilde{M}^R] \quad , \quad [\tilde{K}] = [K^C] + [\tilde{K}^R] \quad (26)$$

$$[K^C] = \sum_{i=1}^p \left(\frac{u_i + l_i}{2} \right) [\bar{K}_i]^e \quad , \quad [M^C] = \sum_{i=1}^p \left(\frac{u_i + l_i}{2} \right) [\bar{M}_i]^e \quad (27)$$

$$[\tilde{K}^R] = \sum_{i=1}^p (\varepsilon_i) \left(\frac{u_i - l_i}{2} \right) [\bar{K}_i]^e \quad , \quad [\tilde{M}^R] = \sum_{i=1}^p (\varepsilon_i) \left(\frac{u_i - l_i}{2} \right) [\bar{M}_i]^e \quad (28)$$

where $[K^C]$ and $[M^C]$ represent the matrices of mean values, $[\tilde{M}^R]$ and $[\tilde{K}^R]$. represent the radial matrices, $[l_i, u_i]$ is the numerical interval of each element that forms the interval matrix and ε_i is the interval coefficient.

The determination of the limits of natural frequencies and modes shape in the presence of interval uncertainties is interpreted mathematically as an eigenvalue problem centered on the matrices $[K^C]$ an $[M^C]$ and subject to radial perturbations represented by the matrices $[\tilde{M}^R]$ and $[\tilde{K}^R]$. This perturbation is obtained by the linear sum of the deterministic matrices $[\bar{M}_i]^e$ and $[\bar{K}_i]^e$ of the element multiplied by an interval coefficient ε_i .

$$\tilde{\lambda}([\tilde{K}], [\tilde{M}]) = \left(\frac{\{x\}^T [\tilde{K}]\{x\}}{\{x\}^T [\tilde{M}]\{x\}} \right) = \left(\frac{\{x\}^T [K^C] + [\tilde{K}^R]\{x\}}{\{x\}^T [M^C] + [\tilde{M}^R]\{x\}} \right) \quad (29)$$

$$\frac{\{x\}^T [K^C] + [\tilde{K}^R]\{x\}}{\{x\}^T [M^C] + [\tilde{M}^R]\{x\}} = \frac{\sum_{i=1}^p \left(\frac{u_i + l_i}{2} \right) \{x\}^T [\bar{K}_i]^e \{x\} + \sum_{i=1}^p (\varepsilon_i) \left(\frac{u_i - l_i}{2} \right) \{x\}^T [\bar{K}_i]^e \{x\}}{\sum_{i=1}^p \left(\frac{u_i + l_i}{2} \right) \{x\}^T [\bar{M}_i]^e \{x\} + \sum_{i=1}^p (\varepsilon_i) \left(\frac{u_i - l_i}{2} \right) \{x\}^T [\bar{M}_i]^e \{x\}} \quad (30)$$

Since $[K^C]$ is a symmetric positive semidefinite matrix (as $\{x\}^T [K^C]\{x\} \geq 0$), then, $[K^C]$ matrix will be subject to perturbation of a symmetric positive semidefinite matrix $[\tilde{K}^R]$. Whereas, $[M^C]$ symmetric positive definite matrix (as $\{x\}^T [M^C]\{x\} > 0$) will be subject to perturbation of a symmetric positive definite matrix $[\tilde{M}^R]$, according to $(\{x\}^T [\tilde{M}^R]\{x\} > 0)$.

Eigenvalues of an interval dynamic system can be solved using the concept of maximum-minimum characterization of the eigenvalues formed by symmetric matrices, as shown in equations (31) and (33).

The first interval eigenvalue is calculated by:

$$\tilde{\lambda}_i([\tilde{K}], [\tilde{M}]) = \min_{\substack{\{x\} \in \mathbb{R}^p \\ \{x\} \neq \{0\}}} \left(\frac{\{x\}^T [K^C] + [\tilde{K}^R]\{x\}}{\{x\}^T [M^C] + [\tilde{M}^R]\{x\}} \right) \quad (31)$$

$$\min[\tilde{\lambda}_i([\tilde{K}], [\tilde{M}])] = \left[\frac{\sum_{i=1}^p \left(\frac{u_i + l_i}{2} \right) \{x\}^T [\bar{K}_i]^e \{x\} - \sum_{i=1}^p \left(\frac{u_i - l_i}{2} \right) \{x\}^T [\bar{K}_i]^e \{x\}}{\sum_{i=1}^p \left(\frac{u_i + l_i}{2} \right) \{x\}^T [\bar{M}_i]^e \{x\} + \sum_{i=1}^p \left(\frac{u_i - l_i}{2} \right) \{x\}^T [\bar{M}_i]^e \{x\}} \right] \quad (32)$$

and the others by:

$$\tilde{\lambda}_i([\tilde{K}], [\tilde{M}]) = \max_{\substack{\{x\}^T \{s_i\} = \{0\} \\ i=1, \dots, p \\ \{x\} \neq \{0\}}} \left(\frac{\{x\}^T [K^C] + [\tilde{K}^R]\{x\}}{\{x\}^T [M^C] + [\tilde{M}^R]\{x\}} \right) \quad (33)$$

$$\max [\tilde{\lambda}_i([\tilde{K}], [\tilde{M}])] = \frac{\sum_{i=1}^p \left(\frac{u_i + l_i}{2} \right) \{x\}^T [\bar{K}_i]^e \{x\} + \sum_{i=1}^p \left(\frac{u_i - l_i}{2} \right) \{x\}^T [\bar{K}_i]^e \{x\}}{\sum_{i=1}^p \left(\frac{u_i + l_i}{2} \right) \{x\}^T [\bar{M}_i]^e \{x\} - \sum_{i=1}^p \left(\frac{u_i - l_i}{2} \right) \{x\}^T [\bar{M}_i]^e \{x\}} \quad (34)$$

Upper and lower bounds of the natural frequencies of a dynamic problem with interval parameters can be calculated by means of pseudo-deterministic eigenvalue problem, as equations (35) and (36).

$$\sum_{i=1}^p (l_i) [\bar{K}_i]^e \{x\} = (\omega_{\min}^2) \sum_{i=1}^p (u_i) [\bar{M}_i]^e \{x\} \quad (35)$$

$$\sum_{i=1}^p (u_i) [\bar{K}_i]^e \{x\} = (\omega_{\max}^2) \sum_{i=1}^p (l_i) [\bar{M}_i]^e \{x\} \quad (36)$$

Results

Beam

The objective in case 1 is to evaluate the execution time of the program developed in MATLAB[®] due to the increase in the number of elements of stepped beams, as Figure 1. The elements of case 1 were adopted dimensionless (unitary) parameters, such as specific mass, length, cross-sectional area and area moment of inertia. The modulus of elasticity parameters was adopted intervals and dimensionless (as). The curve of execution time grows by increasing the number of elements and the degree of freedom (DOF), as shown in Figure 2. The growth curve follows a logarithmic function.

Truss with three bar elements

A truss formed by 3 elements of bars and 2 degrees of effective freedom is presented with imprecision in its elasticity modules, as Figure 3. The dimensionless natural frequencies are given by equation (37) and the bounds of the frequency range are obtained by equations (39) and (40).

$$\Omega_i = \omega_i L \sqrt{\frac{\rho}{E}} \quad (37)$$

As mentioned, the generalized eigenvalue problem for dynamic systems is given by:

$$([K] - (\lambda)[M])\{x\} = \{0\} \quad (38)$$

where, ω is the eigenvalue, ω , is the natural frequency, $[K]$, is the mode shape (or eigenvector), $[K]$ is the global stiffness matrix and $[M]$ the global mass matrix.

The problem of pseudo-deterministic eigenvalue formulated for the truss of Figure 3, in the presence of uncertainties in the modulus of elasticity of two of the barelements, as $\tilde{E}_1 = [E_1^l; E_1^u] = ([0, 85; 1, 1])E$

(first bar element) and $\tilde{E}_3 = [E_3^l; E_3^u] = ([1; 1])E$ (second element).

The third element has unitary value, as $\tilde{E}_3 = [E_3^l; E_3^u] = ([1; 1])E$.

$$\left(\frac{A}{4L} \begin{bmatrix} E_1^u + E_3^u & \sqrt{3}E_1^u - \sqrt{3}E_3^u & -E_3^u \\ \sqrt{3}E_1^u - \sqrt{3}E_3^u & 3E_1^u + 3E_3^u & \sqrt{3}E_3^u \\ -E_3^u & \sqrt{3}E_3^u & 4E_1^u + E_3^u \end{bmatrix} - (\omega_{\max}^2)\rho AL \begin{bmatrix} 1 & 0 & 0 \\ 0 & 1 & 0 \\ 0 & 0 & 1 \end{bmatrix} \right) \begin{Bmatrix} x_3 \\ x_4 \\ x_6 \end{Bmatrix} = \begin{Bmatrix} 0 \\ 0 \\ 0 \end{Bmatrix} \quad (39)$$

$$\left(\frac{A}{4L} \begin{bmatrix} E_1^l + E_3^l & \sqrt{3}E_1^l - \sqrt{3}E_3^l & -E_3^l \\ \sqrt{3}E_1^l - \sqrt{3}E_3^l & 3E_1^l + 3E_3^l & \sqrt{3}E_3^l \\ -E_3^l & \sqrt{3}E_3^l & 4E_1^l + E_3^l \end{bmatrix} - (\omega_{\min}^2)\rho AL \begin{bmatrix} 1 & 0 & 0 \\ 0 & 1 & 0 \\ 0 & 0 & 1 \end{bmatrix} \right) \begin{Bmatrix} x_3 \\ x_4 \\ x_6 \end{Bmatrix} = \begin{Bmatrix} 0 \\ 0 \\ 0 \end{Bmatrix} \quad (40)$$

Table 1 presents the natural frequencies defined dimensionless by equation (37), whose unitary values are $L = A = \rho = E = 1$.

Truss with ten bar elements

The objective in case 3 is evaluate the degree of overestimation of a truss is formed by ten bar elements, with two DOF by node and a total of nine effective DOF, as in Figure 4.

Area interval parameters were adopted for the following elements: 1, 2, 3, 4 and 6. The intervals vary proportionally to the uncertainty factor β within the range $0 \leq \beta \leq 3\%$, as equation (41).

$$A_i^l = [A^c - \beta A^c; A^c + \beta A^c] \quad (41)$$

where $i=1,2,3,4,6$, the area mean value is $A^c = 1,0$ and β vary into the range $0 \leq \beta \leq 3\%$.

The evaluation of the degree of overestimation is done by comparing the results obtained by the author's method, perturbation theory of matrices, as Figure 5a, with the results obtained by the Monte Carlo Method as Figure 5b.

The resulting eigenvalues from Figures 5a and 5b increases as the range of the input parameter of the problem increases. The resulting ranges of the eigenvalues obtained by Monte Carlo are narrower than those obtained by the author, which indicates an acceptable overestimation when the interval magnitude increases.

Figure 5 shows the behavior of the overestimation of the results with increasing the range of eigenvalues, as the area uncertainty factor assumes increasing values in the interval $0 \leq \beta \leq 3\%$. The increase in the overestimation of the results follows an increasing linear function, as the range of truss input parameters increase, as shown in the Figures 5a and 5b. Figure 6a shows the behavior of the overestimation in the presence of the lower bounds of the interval parameters. Figure 6b refers to overestimation in the presence of the upper bounds of the parameters.

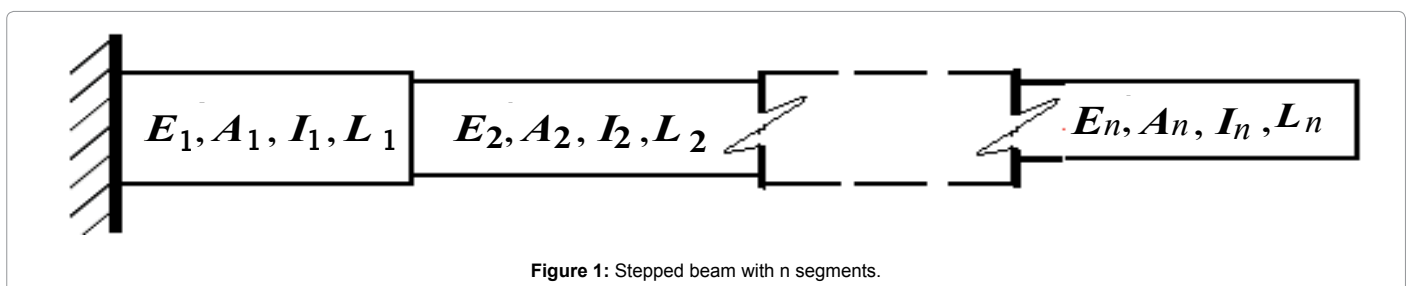


Figure 1: Stepped beam with n segments.

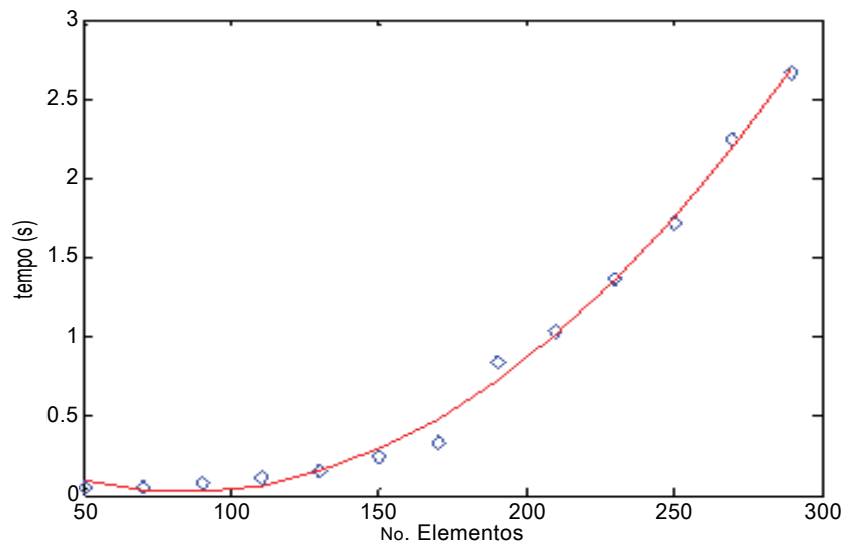


Figure 2: Behavior of the curve of the computation time of the algorithm developed for a stepped beam with interval parameters.

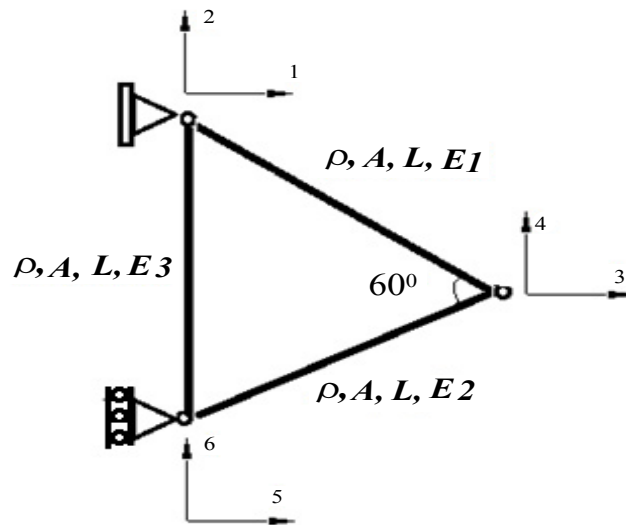


Figure 3: Truss with three bar elements.

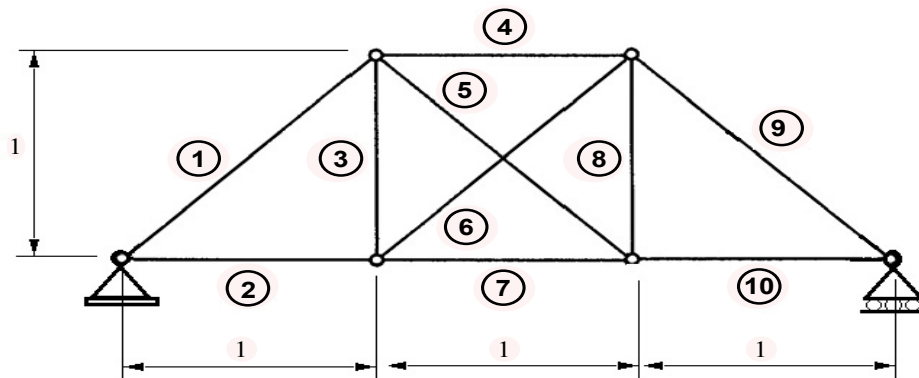
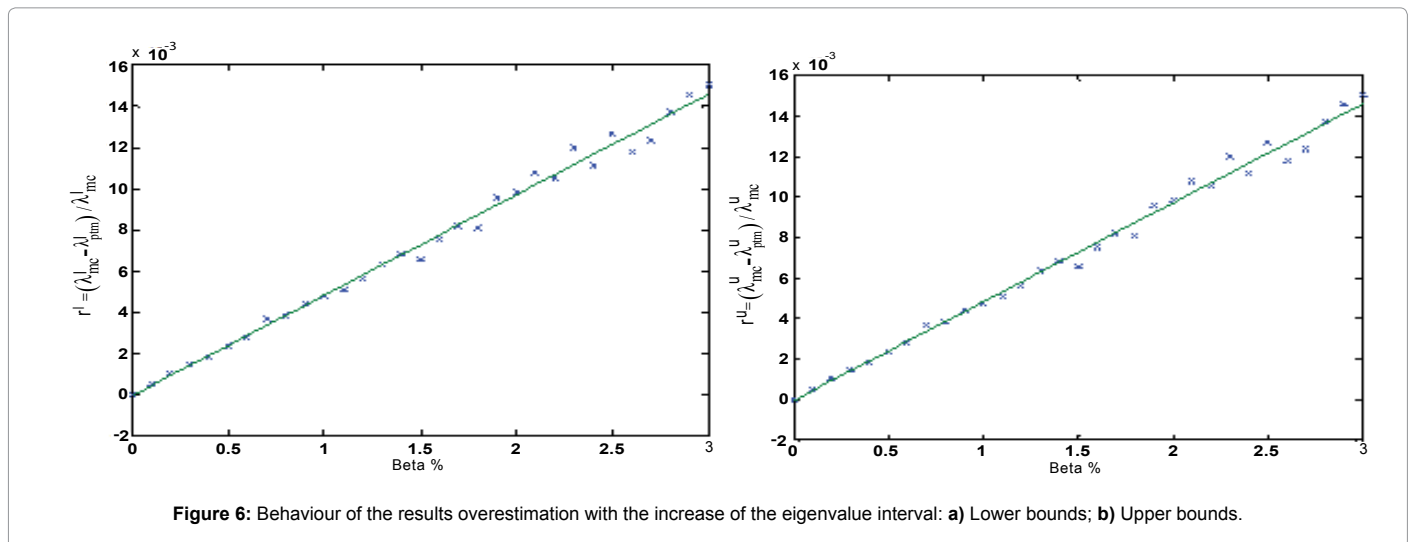
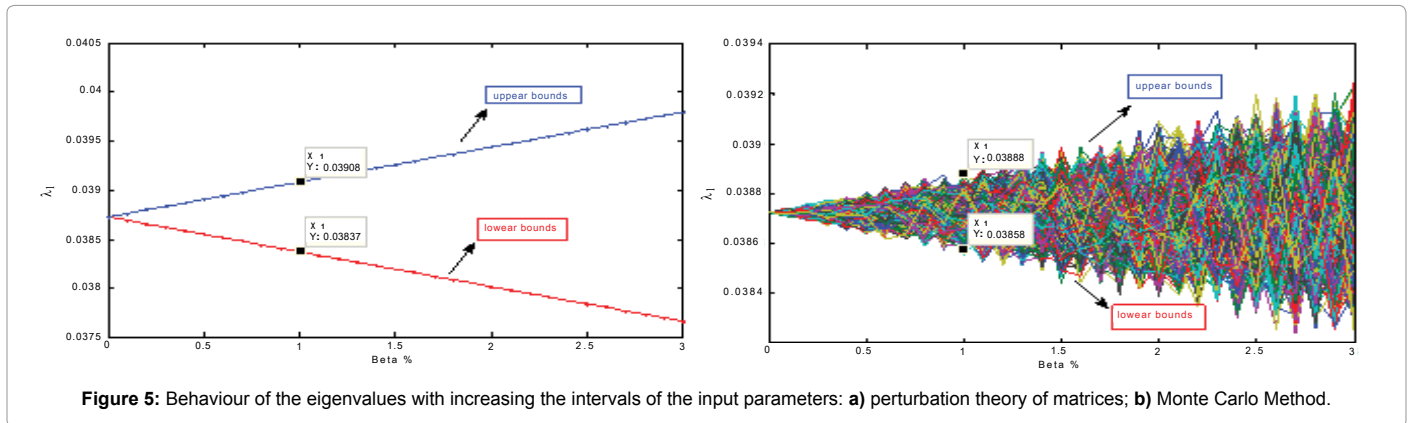


Figure 4: Truss with ten bar elements.



| Interval dimensionless natural frequencies | | |
|---|-------------|-------------|
| $\tilde{E}_1 = [E_1^l; E_1^u] = ([0.85; 1.1])E$ | | |
| $\tilde{E}_2 = [E_2^l; E_2^u] = ([0.75; 1.4])E$ | | |
| $\tilde{E}_3 = [E_3^l; E_3^u] = ([1; 1])E$ | | |
| | Lower bound | Upper bound |
| Ω_1 | 0.7723 | 0.9578 |
| Ω_2 | 1.3429 | 1.6830 |

Table 1: Dimensionless natural frequencies of a truss formed by three bar elements with interval modulus of elastic.

The vertical axis of graphic r^i is the relative difference of the eigenvalues obtained by the author with those obtained by Monte Carlo, as Figure 5. The relative difference is calculated by:

$$r^i = \frac{\lambda_{mc}^i - \lambda_{ptm}^i}{\lambda_{mc}^i} \quad (42)$$

Where $i=l,u$ is the superscript index, l is the index of lower bounds of the eigenvalue λ_{mc}^u and λ_{mc}^l , u is the index of upper bounds of λ_{mc}^u and λ_{ptm}^l . The eigenvalue λ_{ptm}^i is calculated by author using

the Perturbation Theory of Matrix (PTM) and λ_{mc}^i is the eigenvalue calculated by Monte Carlo (MC) simulation.

For example: The Figures 6a and 6b was obtained from eigenvalues of the first natural frequency of truss shown in Figure 3. The example shown in Table 2 is for eigenvalues obtained with $\beta = 1\%$.

Frame

The case 4 refers to a frame with 14 elements, 15 nodes and 39 effective degrees of freedom, as Figure 7.

The frame elements 1, 2, 6, 12 and 13 were adopted with uncertainties in the cross-sectional area and at the moment of inertia, the other parameters are considered with fixed values, such as the specific mass $E = 200$ GPa, the modulus of elasticity $E = 200$ GPa, as Table 3. All the elements were adopted with length of 0.2 m. Table 4 shows the eigenvalues for a frame with the interval parameters from Table 3.

Discussion and Conclusion

This article presents a methodology for the evaluation of the influence of the interval parameters on the dynamic response of a system using the finite element method. A computational program was developed using the Perturbation Theory of Matrices due the capability to generate reliable results in a short period of time and

| Relations | Lower bound $\beta = 1\%$ | Upper bound $\beta = 1\%$ |
|---|--|--|
| Eigenvalues by Perturbation Theory of Matrix $\lambda_{ptm} = [\lambda_{ptm}^l; \lambda_{ptm}^u]$ | $\lambda_{ptm}^l = 0.03837$ | $\lambda_{ptm}^u = 0.03908$ |
| Eigenvalues by Monte Carlo Method $\lambda_{mc} = [\lambda_{mc}^l; \lambda_{mc}^u]$ | $\lambda_{mc}^l = 0.03857$ | $\lambda_{mc}^u = 0.03886$ |
| $r_{\beta=1\%}^{l,u} = \frac{\lambda_{mc}^{l,u} - \lambda_{ptm}^{l,u}}{\lambda_{mc}^{l,u}}$ | $r_{\beta=1\%}^l = 5.185 \times 10^{-3}$ | $r_{\beta=1\%}^u = 7.463 \times 10^{-3}$ |

Table 2: Relative differences of eigenvalues (for truss shown in Figure 3) with numerical interval in $\beta=1\%$.

| Frame elements | Moment of inertia $\tilde{I} = [I^l; I^u]$ (m ⁴) | Cross-sectional area $\tilde{A} = [A^l; A^u]$ (m ²) | Specific mass ρ (kg/m ³) | Modulus of elasticity E(GPa) |
|---------------------------------|---|--|--|---------------------------------|
| 1 and 12 | $[0.0999; 0.1001] \times 10^{-4}$ | $[0.99; 1.01] \times 10^{-2}$ | 7,800 | 200 |
| 2 and 13 | $[0.1998; 0.2002] \times 10^{-4}$ | $[1.426; 1.454] \times 10^{-2}$ | 7,800 | 200 |
| 6 | $[0.04995; 0.05005] \times 10^{-4}$ | $[0.634; 0.646] \times 10^{-2}$ | 7,800 | 200 |
| 3, 4, 5, 7, 8, 9, 10, 11 and 14 | $[0.1; 0.1] \times 10^{-4}$ | $[1.0; 1.0] \times 10^{-2}$ | 7,800 | 200 |

Table 3: Physical and geometric parameters of each element of the frame shown in Figure 5.

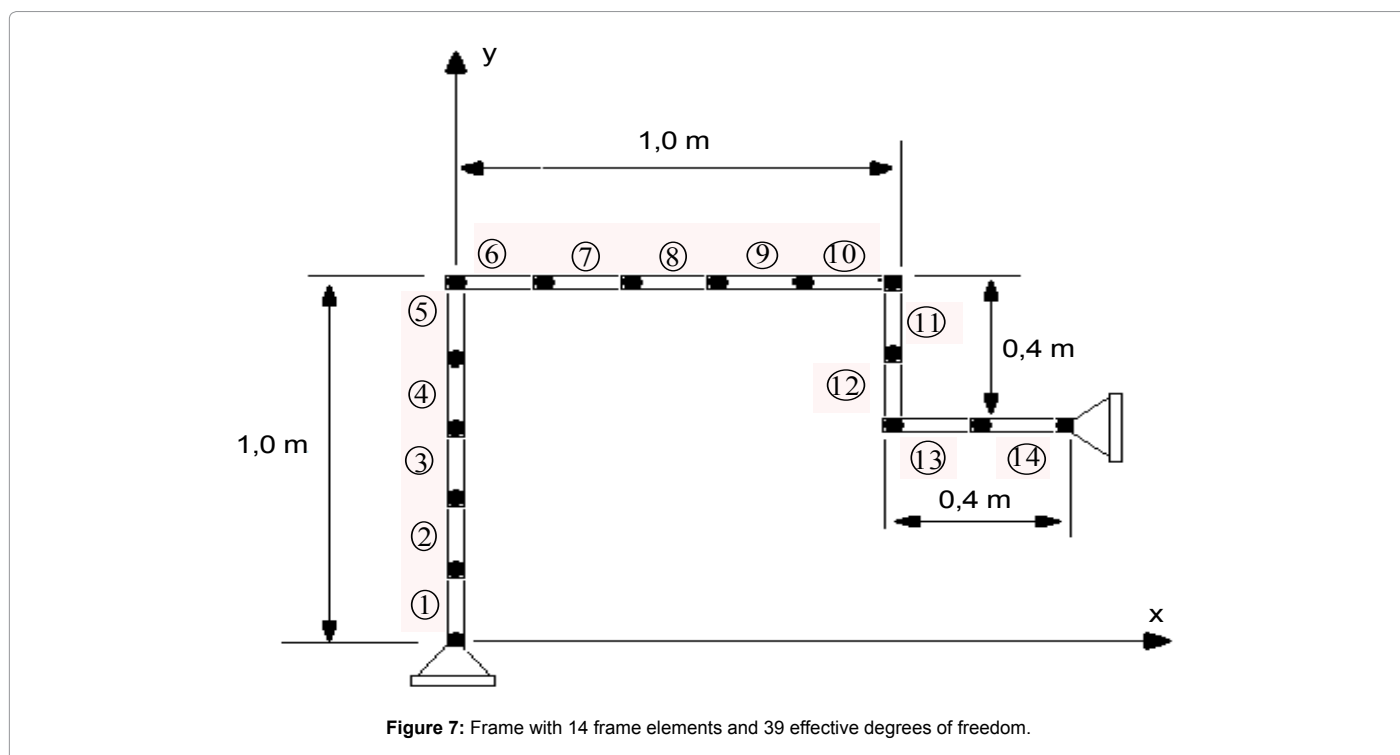


Figure 7: Frame with 14 frame elements and 39 effective degrees of freedom.

| Eigen-values | | |
|---------------------|------------------------------------|------------------------------------|
| Interval parameters | | |
| λ | Lower bound | Upper bound |
| λ_1 | 5.9953668744×10^5 | 6.0137826935×10^5 |
| λ_2 | $3.47510348019 \times 10^6$ | $3.49523222982 \times 10^6$ |
| λ_3 | $6.52479786731 \times 10^6$ | $6.57035253351 \times 10^6$ |
| λ_4 | $1.162146631440 \times 10^7$ | $1.168281940056 \times 10^7$ |
| λ_5 | $4.544173616292 \times 10^8$ | $4.593217098825 \times 10^7$ |
| λ_6 | $6.634489763163 \times 10^7$ | $6.709407442299 \times 10^7$ |
| λ_7 | $8.950821154738 \times 10^7$ | $9.024151720400 \times 10^7$ |
| λ_8 | $1.3206006855737 \times 10^5$ | $1.3369356349779 \times 10^8$ |
| λ_9 | $2.1353188654430 \times 10^8$ | $2.1572270914742 \times 10^8$ |
| λ_{10} | $2.5192569919679 \times 10^8$ | $2.5455604858173 \times 10^8$ |
| λ_{11} | $2.8968728951151 \times 10^8$ | $2.9405708216015 \times 10^8$ |
| λ_{12} | $3.7498304982751 \times 10^8$ | $3.7800804912494 \times 10^8$ |
| λ_{13} | $4.6042133013289 \times 10^8$ | $4.6676538425856 \times 10^8$ |
| λ_{14} | $5.4960180414309 \times 10^8$ | $5.5613219566965 \times 10^8$ |
| λ_{15} | $7.3108465622893 \times 10^8$ | $7.3754708830533 \times 10^8$ |
| λ_{16} | $9.0738638440035 \times 10^8$ | $9.1569639401521 \times 10^8$ |
| λ_{17} | $1.10147237064439 \times 10^9$ | $1.11347748038401 \times 10^9$ |
| λ_{18} | $1.23722073989728 \times 10^9$ | $1.25036373970076 \times 10^9$ |
| λ_{19} | $1.68705672505858 \times 10^9$ | $1.70602654046057 \times 10^9$ |
| λ_{20} | $1.87999570173437 \times 10^9$ | $1.89623047878967 \times 10^9$ |
| λ_{21} | $2.35821044409556 \times 10^9$ | $2.37873493434071 \times 10^9$ |
| λ_{22} | $3.03381937642706 \times 10^9$ | $3.06819802648441 \times 10^9$ |
| λ_{23} | $3.22251612516316 \times 10^9$ | $3.25944452451049 \times 10^9$ |
| λ_{24} | $3.73926431274539 \times 10^9$ | $3.78778111550643 \times 10^9$ |
| λ_{25} | $4.20211104046095 \times 10^9$ | $4.26150597423892 \times 10^9$ |
| λ_{26} | $4.25630059483613 \times 10^9$ | $4.31618058211313 \times 10^9$ |
| λ_{27} | $5.10086811426856 \times 10^9$ | $5.16897664243100 \times 10^9$ |
| λ_{28} | $6.20177347213656 \times 10^9$ | $6.27957979811479 \times 10^9$ |
| λ_{29} | $6.44404396987963 \times 10^9$ | $6.48339725184557 \times 10^9$ |
| λ_{30} | $6.90506093550566 \times 10^9$ | $6.95302049322776 \times 10^9$ |
| λ_{31} | $7.61520284922480 \times 10^9$ | $7.68565194468737 \times 10^9$ |
| λ_{32} | $9.14530811665328 \times 10^9$ | $9.24847772302015 \times 10^9$ |
| λ_{33} | $2.21716325969128 \times 10^{10}$ | $1.228471235319194 \times 10^{10}$ |
| λ_{34} | $1.539181431226008 \times 10^{10}$ | $1.549099926167509 \times 10^{10}$ |
| λ_{35} | $2.272488653930983 \times 10^{10}$ | $2.283519484706917 \times 10^{10}$ |
| λ_{36} | $2.858065763586156 \times 10^{10}$ | $2.885843311641310 \times 10^{10}$ |
| λ_{37} | $3.307753932142422 \times 10^{10}$ | $3.334788706501518 \times 10^{10}$ |
| λ_{38} | $3.933228048294351 \times 10^{10}$ | $3.962897443669482 \times 10^{10}$ |
| λ_{39} | $4.317287636191113 \times 10^{10}$ | $4.357233362051358 \times 10^{10}$ |

Table 4: Interval eigenvalues for the frame of Figure 5.

| Edge geometry | Regression equation |
|---------------|--|
| LH | $-0.269 - 0.008285 \times V_c + 8.009 \times f - 3.142 \times a_p + 0.01230 \times H + 0.000189 \times V_x - 0.000014 \times V_z + 0.03249 \times V_c \times a_p - 0.001161 \times f \times V_x$ |
| HH | $-0.2468 - 0.008285 \times V_c + 6.979 \times f - 3.142 \times a_p + 0.01354 H + 0.000189 \times V_x - 0.000014 \times V_z + 0.03249 \times V_c \times a_p - 0.001161 \times f \times V_x$ |
| W | $0.4039 - 0.008285 \times V_c + 2.276 \times f - 3.142 \times a_p + 0.00508 H + 0.000189 V_x - 0.000014 V_z + 0.03249 V_c \times a_p - 0.001161 \times f \times V_x$ |

Table 5: Regression models for different tool edge geometries.

| S. No | Number of neurons in the hidden layer | MSE |
|-------|---------------------------------------|----------|
| 1 | 10 | 0.00126 |
| 2 | 15 | 0.000835 |
| 3 | 19 | 0.000724 |
| 4 | 25 | 0.000951 |
| 5 | 32 | 0.00987 |

Table 6: Number of neurons in hidden layer and MSE.

| S. No | Training function | MSE | Epochs |
|-------|-------------------|-----------|--------|
| 1 | Train br | 0.0009752 | 9 |
| 2 | Train lm | 0.000724 | 4 |
| 3 | Training dx | 0.0010957 | 12 |
| 4 | Train rp | 0.0007958 | 7 |

Table 7: Different training functions and MSE.

| Average % error | | | | | |
|-----------------|---------|--------------|--------------|----------|--------|
| Expt No | Ra-Expt | Ra-ANN (tst) | Ra-Reg (tst) | Ra (Reg) | Ra ANN |
| 8 | 0.75 | 0.7465 | 0.76 | 1.33 | 0.46 |
| 15 | 0.16 | 0.1624 | 0.15 | 6.25 | 1.50 |
| 22 | 0.48 | 0.4792 | 0.49 | 2.08 | 0.16 |
| 34 | 0.8 | 0.796 | 0.82 | 2.5 | 0.50 |
| 44 | 0.16 | 0.1624 | 0.15 | 6.25 | 1.50 |
| -- | -- | -- | MAPE | 3.68 | 0.82 |

Table 8: Experimental and predicted values of surface roughness for testing data.

| MAPE for training data | |
|------------------------|--------|
| Regression analysis | ANN |
| 4.622 | 0.6401 |

Table 9: Mean absolute percent error for regression and ANN.

with great possibility of application in practice. In case 1 observed that the slope of the curve of Figure 2 shows a growth of the computation time with the increase of the number of elements and the DOF (Tables 5-9). The growth curve follows a logarithmic function. In case 2, the dimensionless natural frequencies were presented for a truss. In case 3, the increase in the overestimation of the results follows an increasing linear function, as the range of truss input parameters increase within the range. The case 4 refers to a frame with 14 elements, 15 nodes and 39 effective degrees of freedom. The eigenvalues behavior was evaluated in the presence of uncertainties in the cross-sectional area and the moment of inertia.

Declaration of conflicting interests

The author(s) declared no potential conflicts of interest with respect to the research, authorship, and/or publication of this article.

Funding

The authors are grateful to the financial support from FAPEMIG (Research Foundation of the State of Minas Gerais) by Proc. TEC-1670/05 and from CAPES (Coordination of Improvement of Higher Education Personnel) by scholarship support.

References

- Oberkampf W, Deland S, Rutherford B, Diegert K, Alvin K (1999) A new methodology for the estimation of total uncertainty in computational simulation. *Struct Dyn and Mater Conf* 4: 99-1612.
- Burkill JC (1924) Functions of intervals. *Proceedings of the London Mathematical Society* 22: 375-446.
- Sunaga T (2009) Theory of interval algebra and its application to numerical analysis. *JJIAM* 26: 125-143.
- Landowski M (2015) Differences between Moore and RDM interval arithmetic. *AISC*.
- Moore RE (1962) Interval arithmetic and automatic: Analysis in Digital Computing.
- Matos JC(2007) Treatment of uncertainties in numerical models in civil engineering.
- Matsumoto M, Iwaya E (2000) Interval finite element analysis to structural systems. *IEEE international workshop on robot and human interactive communication, Japan*.
- Pereira SC (2002) A uncertainty treatment in basin modeling. *Tese De Doutorado. Federal University of Rio De Janeiro, Brazil*.
- Qiu Z, Wang X, Friswell MI (2005) Eigenvalue bounds of structures with uncertain-but-bounded parameters. *J Sound Vib* 282: 297-312.
- Wang Z, Tian Q, Hu H (2015) Dynamics of spatial rigid-flexible multibody systems with uncertain interval parameters. *Springer Sci* 84: 527-548.